Fatigue Behavior of Steel Fiber Concrete in Direct Tension

Benard Isojeh, S.M.ASCE[1]; Maria El-Zeghayar, Ph.D.[2]; and Frank J. Vecchio, Ph.D., P.Eng., M.ASCE[3]

Abstract: An investigation was conducted to study the behavior of plain concrete and steel fiber reinforced concrete under direct tension fatigue loading. Tests were conducted on dogbone specimens with varying amounts of steel fiber volume content (0, 0.75, and 1.5%). A new concept was introduced in deriving material damage parameters for plain and steel fiber concrete. The parameters developed were implemented into a damage evolution function to enable the prediction of concrete strength and fatigue secant modulus deterioration of steel fiber reinforced concrete. As such, the damage evolution models developed for steel fiber concrete can be implemented into steel fiber reinforced concrete constitutive models for the analysis of fatigue-damaged concrete elements. From the experimental results, the deformation profiles for plain and steel fiber concrete were similar, and the well-known relationship between the fatigue life and secondary strain rate of concrete in compression also exist for plain concrete and steel fiber concrete in tension. In addition, under the same loading parameters, the fatigue life of steel fiber concrete was found to increase as steel fiber content increased from 0 to 1.5%. **DOI: 10.1061/(ASCE)MT.1943-5533.0001949.** © *2017 American Society of Civil Engineers.*

Introduction

The deterioration of a concrete element evolves as cracked planes emanate in concrete under fatigue loading. In reinforced concrete elements, the initiation of macrocracks results in localized stress increments in the embedded reinforcement. Depending on the magnitude of the induced stress, a crack may initiate on a reinforcing bar at its intersection with the cracked concrete plane and subsequent fatigue loading cycles may result in widening of concrete cracks. Ultimately, fracture of the reinforcement may occur as the reinforcing bar cracks propagate.

The presence of concrete cracks and excessive opening under fatigue loading may result in serious durability issues such as accelerated reinforcement crack growth (attributable to corrosive environment) and reduced stiffness of the overall structural element. As such, a majority of fatigue-prone concrete structures such as highways, airport pavements, and offshore structures are usually designed to ensure cracking of concrete is held to a minimum (Vega et al. 1995; Guo 2014).

Because cracks are inevitable in some concrete structures, developing a means of ensuring their evolution are prevented by crack-bridging is imperative. However, designs of fatigue-prone concrete structures against cracking under tensile fatigue loading require adequate knowledge of the fatigue life of concrete in tension and its corresponding deformation evolutions.

Reports in the literature have shown that steel fiber possesses crack-bridging attributes which restrain the opening of cracks under fatigue loading. As such, its use has been employed in various structural elements such as concrete pavements, bridge decks, and machine foundations (Zhang et al. 1999). Experimental investigations on steel fiber concrete portraying crack-bridging and enhanced fatigue life attributes have been reported in the literature using flexural fatigue tests on steel fiber concrete prisms. Tests reported by Ramakrishnan et al. (1989), Chenkui and Guofan (1995), Nanni (1991), Chang and Chai (1995), and Naaman and Hammoud (1998) all indicate enhanced fatigue life through crack arrests.

To predict the fatigue life of plain concrete elements, stress-life models have been developed in the literature for concrete under tension and compression fatigue loading (Tepfers 1979; Oh 1986; Torrenti et al. 2010; FIB 2010). Such models relate the ratio of the maximum stress level (ratio of applied stress to concrete strength) to the number of cycles resulting in fatigue failure. However, a concrete material parameter obtained from experiments and other known loading parameters such as the stress ratio (ratio of the minimum stress level to the maximum stress level) is required in such models for reasonable predictions.

Material Parameter in Aas-Jakobsen's S-N Model

It is widely accepted that the Aas-Jakobsen and Lenshow's linear model [Eq. (1)] can be used to estimate the fatigue life of plain concrete in tension, compression, and flexure. The model shows the relationship between the fatigue strength of concrete after a given number of cycles and the ratio of the minimum to maximum stress level. The material parameter (β) required in the model proposed by Aas-Jakobsen and Lenshow (1970) was 0.064. Oh (1986), having conducted flexural tests on plain concrete, proposed a material parameter of 0.069. To account for other plain lightweight concrete, Tepfers and Kutti (1979) proposed a material parameter of 0.0685

$$S_{\max} = 1 - \beta(1 - R)\mathrm{Log}N_f \tag{1}$$

In Eq. (1), $S_{\max}$ = ratio of the maximum stress level to the concrete compressive strength, N_f = number of cycles to failure,

[1]Ph.D. Candidate, Dept. of Civil Engineering, Univ. of Toronto, 35 St George St., Toronto, ON, Canada M5S 1A4 (corresponding author). ORCID: http://orcid.org/0000-0002-5095-5134. E-mail: mb.isojeh@mail.utoronto.ca

[2]Civil Engineer, Renewable Power Business Unit at Hatch Ltd., 4342 Queen St., Niagara Falls, ON, Canada L2E 7J7.

[3]Professor, Dept. of Civil Engineering, Univ. of Toronto, 35 St George St., Toronto, ON, Canada M5S 1A4.

Note. This manuscript was submitted on September 7, 2016; approved on January 24, 2017; published online on May 16, 2017. Discussion period open until October 16, 2017; separate discussions must be submitted for individual papers. This paper is part of the ***Journal of Materials in Civil Engineering***, © ASCE, ISSN 0899-1561.

and R = stress ratio [minimum stress level (σ_{min}) to maximum stress level (σ_{max})].

As a means of predicting the fatigue life of steel fiber concrete using the Aas-Jakobsen's stress-life model, Singh and Kaushik (2001) developed material parameters for steel fiber concrete with fiber volume contents of 0.5, 1, and 1.5% using flexural fatigue tests, obtaining values of 0.0536, 0.0425, and 0.0615, respectively. Although the attempt seems reasonable, the material parameters obtained indicated a lower fatigue life as the steel fiber volume increases from 1.0 to 1.5%. The proposed material parameters also exhibited higher fatigue life for steel fiber concrete with volume content of 0.5% compared with steel fiber concrete with a volume content of 1.5%. These contradict the trend reported by previous investigators (Chang and Chai 1995; Chenkui and Guofan 1995).

As an alternative to the estimation of fatigue life, strain evolution models have been used in the literature. According to Sparks and Menzies (1973), Cornelissen and Reinhardt (1986, 1984) and Taliercio and Gobbit (1996), the fatigue life of a concrete element can be predicted from its strain evolution, because a correlation was found to exist between the secondary strain rate and the number of cycles to failure. From experimental investigations reported in the literature, this approach is not significantly affected by the stochastic influence of concrete. However, the use of such models still requires the fatigue stress levels.

Eq. (1) can be expressed as:

$$\mathrm{Log}(1 - S_{max}) = \mathrm{Log}\beta + V \log(\mathrm{Log}N_f) \tag{2}$$

where $V = (1 - R)k$, and k = constant.

From the correlation between the secondary strain rate and the number of cycles to failure

$$\mathrm{Log}(\mathrm{Log}N_f) = A + B\mathrm{Log}\varepsilon_{sec} \tag{3}$$

where ε_{sec} = secondary strain rate, and A and B are constants to be obtained from experiments. A power law correlation (nonlinear) was initially proposed by Sparks and Menzies (1973); however, the correlation between the number of cycles resulting to fatigue failure and the secondary strain rate is expressed in a linear form [Eq. (3)] by the authors to simplify the analysis required for deriving material parameter β for plain and steel fiber concrete. The corroboration of the model with experimental data is presented in a subsequent section.

A relationship between $\mathrm{Log}(1 - S_{max})$ and the secondary strain rate (ε_{sec}) can be given thus:

$$\mathrm{Log}(1 - S_{max}) = C + D\mathrm{Log}\varepsilon_{sec} \tag{4}$$

C and D are constants obtained from experiments.

From Eqs. (3) and (4)

$$\mathrm{Log}\varepsilon_{sec} = \frac{\mathrm{Log}(\mathrm{Log}\,N_f) - \mathrm{A}}{\mathrm{B}} \tag{5}$$

$$\mathrm{Log}\varepsilon_{sec} = \frac{\mathrm{Log}(1 - \mathrm{Smax}) - \mathrm{C}}{\mathrm{D}} \tag{6}$$

From Eqs. (5) and (6)

$$\mathrm{Log}(1 - S_{max}) = \frac{(\mathrm{CB}) - (\mathrm{AD})}{\mathrm{B}} + \frac{\mathrm{D}}{\mathrm{B}}\mathrm{Log}(\mathrm{Log}N_f)$$

$$T_0 = \frac{(\mathrm{CB}) - (\mathrm{AD})}{\mathrm{B}} \tag{7}$$

By comparing Eqs. (2) and (7), the material parameter required in the S-N model can be obtained thus:

$$\beta = 10^{\mathrm{T}_0} \tag{8}$$

In this investigation, direct tension fatigue tests are conducted using dogbone specimens. The dogbone specimens were initially developed by past researchers at the University of Toronto and elsewhere for direct tension tests under monotonic loading. Herein, the deformation evolution in terms of maximum strain evolution, strain rate, and hysteresis loops are plotted for the given steel fiber volume contents (0, 0.75, and 1.5%). The material constant β is estimated for plain concrete and compared with previous values in the literature. Parameter values are then developed for steel fiber volume contents of 0, 0.75 and 1.5%. In addition, conservative damage models are proposed for the residual strength and fatigue secant modulus of steel fiber concrete.

Experimental Program

Experiments on the fatigue behavior of plain and steel fiber reinforced concrete in direct tension were conducted using dogbone specimens with dimensions of 500 (length) mm × 200 mm × 70 mm. Eight plain concrete specimens and 10 specimens reinforced with 0.75 and 1.5% steel fiber volume content were tested under fatigue loading. Two batches of concrete cast were used for each fiber volume content (0.75 and 1.5%), whereas three batches were cast for plain concrete. At least two dogbones from each cast were tested under monotonic loading before the fatigue tests to observe the average tensile strength per batch. Percentages of the observed tensile strengths were used for the fatigue tests conducted between one and two months after casting. The average tensile strengths are given in Table 1.

A design compressive strength of 50 MPa, having a mix ratio of 1:2:2 and water-cement ratio of 0.5 was used for the cast. The mix ratio represents cement, fine aggregate (fineness modulus 2.6), and

Table 1. Compressive Strength of Plain and Steel Fiber Concrete

Batch number	Average compressive strength (MPa)	Standard deviation for compressive strength	Average tensile strength (MPa)	Steel fiber volume (%)	Date of cast (day/month/year)	Date of test (day/month/year)
1	63.1	1.34	3.5	0	12/11/2015	16/12/2015
2	65.6	0.76	3.6	0	18/11/2015	11/1/2016
3	74.2	2.4	2.7	0	18/3/2016	27/4/2016
4	59.6	3.96	3.2	0.75	22/1/2016	23/2/2016
5	52.2	4.91	3.5	0.75	26/2/2016	31/3/2016
6	51.4	2.04	4.5	1.5	4/3/2016	12/4/2016
7	56.2	3.88	4.1	1.5	11/3/2016	26/4/2016

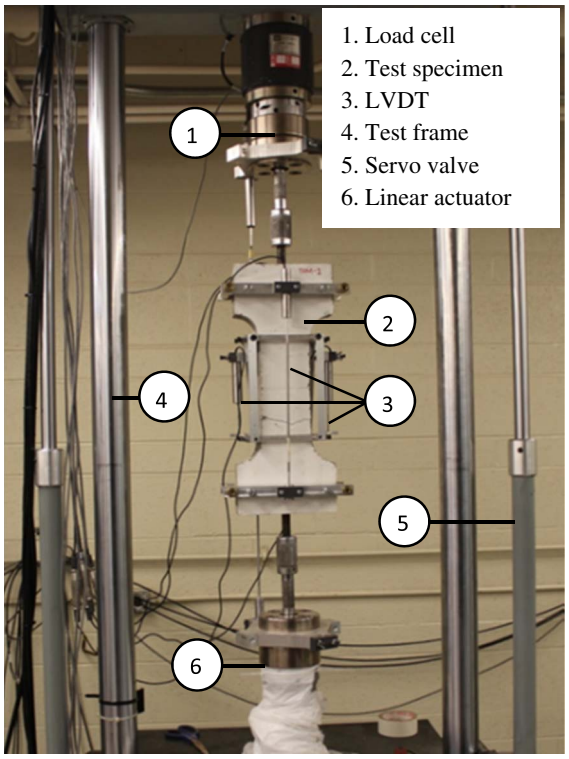

Fig. 1. Test setup

coarse aggregate (10 mm maximum size). High strength end-hooked steel fibers with volume contents of 0.75 and 1.5% (Dramix RC80/30BP) and an ultimate tensile stress capacity of 3,070 MPa were used. The geometrical properties of the fiber included a 30 mm fiber length, a diameter of 0.37 mm, and an aspect ratio of 79. Table 1 also contains the compressive strengths and the corresponding standard deviation per batch of concrete cylinders tested under monotonic loading.

Fig. 1 shows the test setup for the fatigue test in tension. The specimen shown in Fig. 2, specifically for fatigue loading in direct tension, is a modification of dogbone specimens used for direct tension monotonic tests at the University of Toronto. Under monotonic loading, some specimens have been observed to fail because of bond slip between the concrete and the threaded bars. This was prevented by attaching crossbars or anchorage bars to enhance the bond between the concrete and steel reinforcement (Fig. 2). In Fig. 2(a) shows the front elevation of the specimen (wider face), 2(b) shows the side view of the specimen, and 2(c) shows one of the test specimens. LVDTs (linear variable displacement transducers) (attached on the four faces of each specimen) for measuring displacement and the attached mounting rigs are also indicated in Fig. 2.

The tests were conducted using an MTS (material testing systems) servo-hydraulic testing equipment with a loading capacity of 245 kN. The ends of the threaded rods of the dogbone specimens were connected to the testing equipment as shown in Fig. 1. A pulsating load of a continuous sinusoidal waveform which tends to induce tensile stresses in the vertical direction of the specimen was used throughout the investigation. Each specimen was mounted with attached LVDTs as shown in Fig. 2. The LVDTs were used to measure average strains in the specimens throughout the duration of the fatigue tests.

Percentages of the average tensile strengths from the four batches (between 70 and 95%) were used as maximum stress levels for the fatigue tests conducted on plain and steel fiber reinforced concrete dogbones. During fatigue loading, a frequency of 5 Hz (Hertz) and a minimum fatigue load of 2 kN were used for all specimens tested.

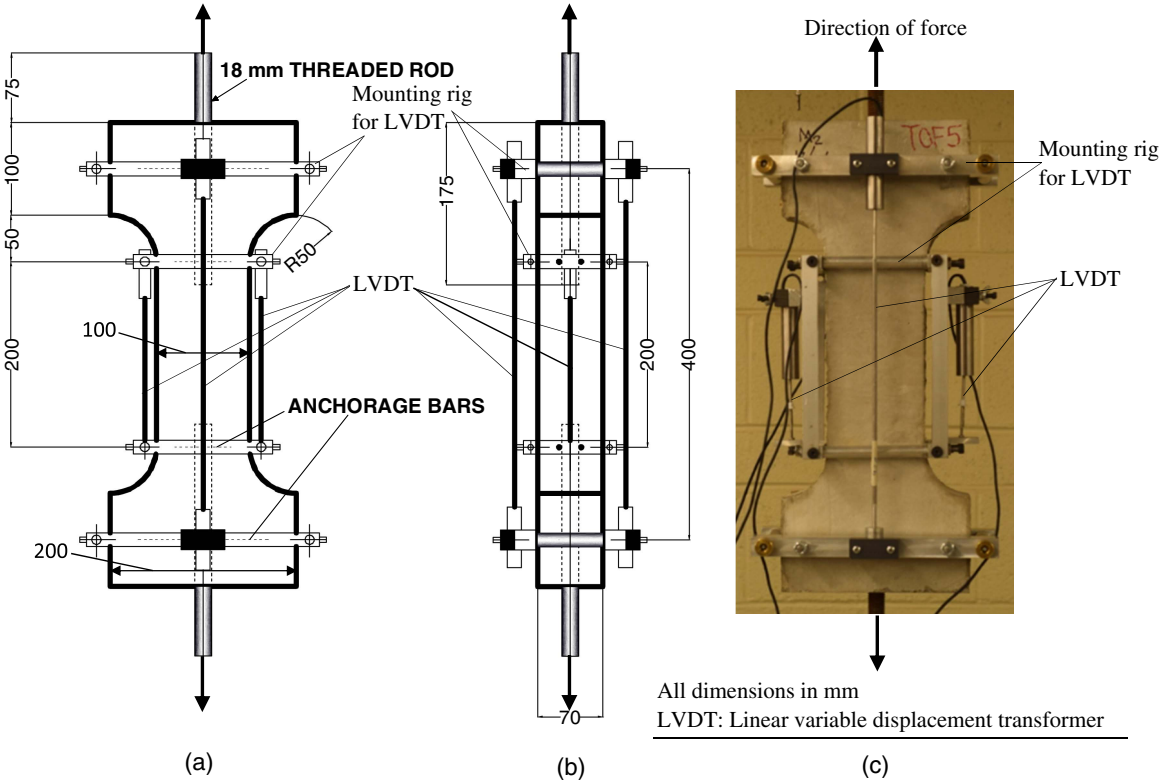

Fig. 2. Test specimen

J. Mater. Civ. Eng., 2017, 29(9): -1--1

Fatigue Results

The results obtained from the experiments are presented in Table 2. The results are subsequently discussed in terms of the failure modes, hysteresis loops, maximum strain evolution, and secondary strain rates.

Table 2. Direct Tension Fatigue Test Results

Specimen name	Steel fiber volume (%)	Stress level	Number of cycles to failure	Secondary strain rate ($\times 10^{-8}$)
TOF1	0	0.79	1,540	1.32
TOF2	0	0.785	1,900	1.23
TOF3	0	0.81	450	4.2
TOF7	0	0.80	641	—
TOF9	0	0.8	4,052	2.04
TKF1	0	0.77	29,269	0.151
TKF3	0	0.733	14,566	0.026
TKF4[a]	0	0.75	21,244	0.10
TT2	0.75	0.766	47,182	0.09
TT4[a]	0.75	0.77	—	—
TT5	0.75	0.903	64	11.1
TT6	0.75	0.82	4,664	0.223
CF1	0.75	0.867	238	8.9
CF2	0.75	0.79	18,335	0.122
CF3	0.75	0.88	302	4.36
CF4	0.75	0.83	1,528	1.35
CF5	0.75	0.90	62	38.9
CF6	0.75	0.81	5,740	0.213
X2	1.5	0.87	915	1.67
X3	1.5	0.8	2,998	0.5
X5	1.5	0.83	4,553	0.186
X6	1.5	0.75	30,391	0.06
X7	1.5	0.78	9,834	0.08
DAB1[a]	1.5	—	200	6.37
DAB2	1.5	0.833	4,326	0.4
DAB3	1.5	0.91	42	28.9
DAB6	1.5	0.857	1,029	1.54
DAB7[a]	1.5	—	736	2.11

[a]Unable to capture deformation data appropriately.

Failure Mode

Under fatigue loading, failure in tension for plain concrete specimens was observed to be localized (discrete). More cracks (smeared) were observed around the failure plane for specimens reinforced with steel fiber (Fig. 3). In all, fracture (separation of each specimen into two parts) occurred at the necked region of each specimen. In some cases, the failure plane coincided with the end of the embedded threaded rod. The estimated applied loading stresses were modified by deducting the cross-sectional area of the threaded rod.

Progressive Deformation

The evolution of the maximum strain were obtained by averaging the LVDT data from the two wide faces of each specimen. As in the case of the maximum strain evolutions obtained for concrete specimens tested under compression fatigue loading (Holmen 1982), the evolution of the maximum strain of concrete tested under tension fatigue loading can also be phased into three stages as reported in the literature. Further, similar evolution profiles were observed for plain and steel fiber reinforced concrete under fatigue loading in direct tension. As shown in Fig. 4, the initial phase portrayed a nonlinear evolution of strain at a decreasing rate (approximately 10–20% of fatigue life).

A constant rate of deformation within a range of approximately 70% of the fatigue life characterized the second phase, whereas the third phase (within 30% of fatigue life) exhibited an increasing rate of damage leading to failure. However, in some steel fiber reinforced concrete specimens, further resistance and increased cycles to failure were observed after sudden increases in deformation within the final phase of damage. This was attributed to crack-bridging of steel fibers between the cracked concrete faces.

In the literature, constitutive models for concrete in tension are usually assumed to be elasto-damage models (Petryna et al. 2002; Maekawa et al. 2006). On the other hand, the behavior of concrete in compression is assumed to be consistent with an elasto-plastic damage model. In Fig. 5, the evolutions of the hysteresis loops of deformation indicate accumulation of irreversible strains from the onset of fatigue loading. The evolutions for plain and steel fiber

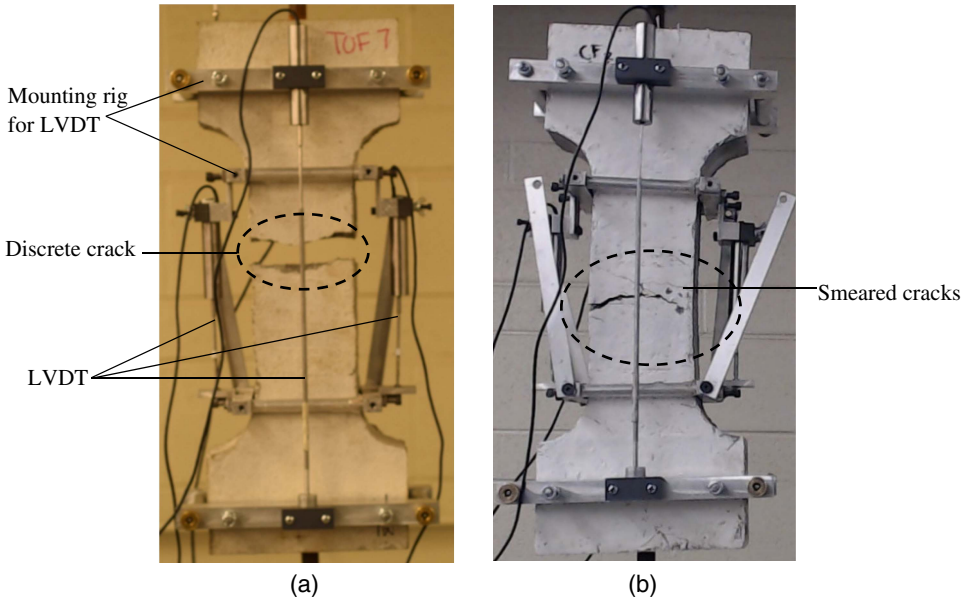

Fig. 3. Test specimens after failure: (a) plain concrete; (b) steel fiber

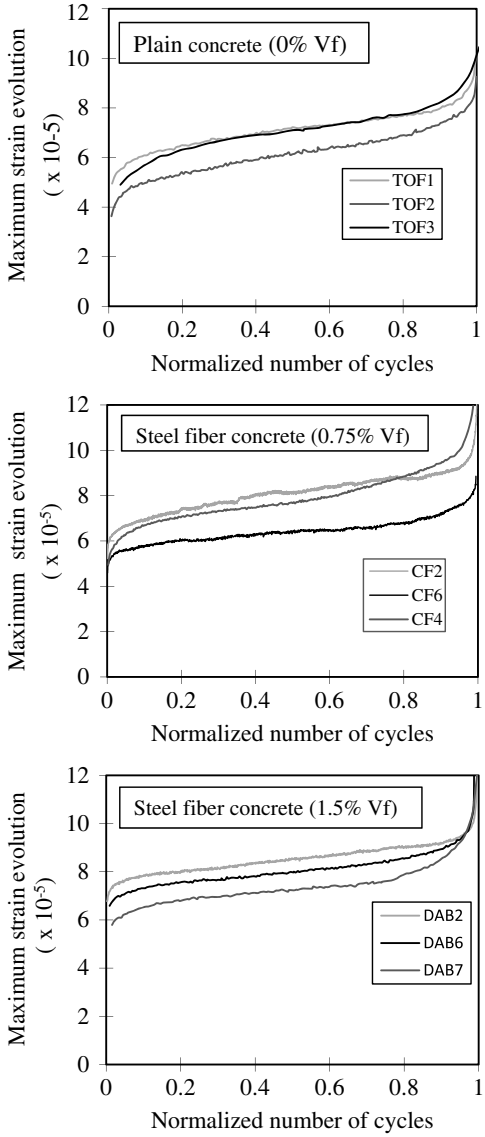

Fig. 4. Fatigue maximum strain evolution for plain and steel fiber concrete

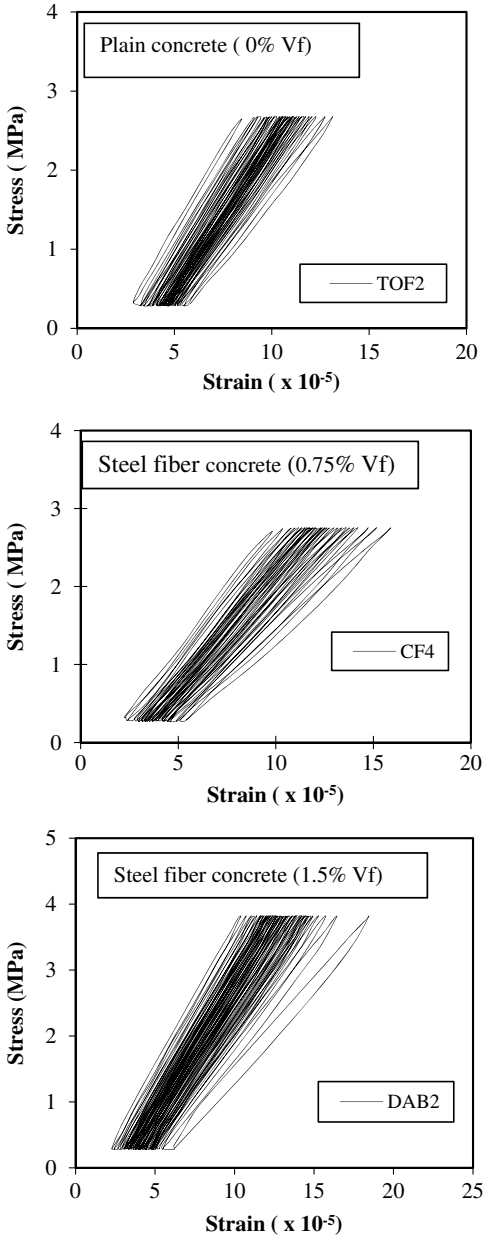

Fig. 5. Fatigue hysteresis loops for plain and steel fiber concrete

reinforced concrete were also observed to be similar. These indicate that the fatigue damage constitutive model for concrete in tension is also elasto-plastic in nature; however, because of the insignificant value of accumulated tensile strains and computation time saved in analysis, the use of elasto-damage models for concrete in tension may be justified.

Although it is well known that the fatigue life of plain concrete in tension and compression are similar, this observation was ascertained to also extend to the profiles of corresponding damage evolutions. Further, the progressive deformations and the damage evolution profiles attributable to fatigue loading of steel fiber concrete specimens were also analogous to those of plain concrete.

Material Parameters for Concrete and Steel Fiber

As previously indicated, the material parameters for plain and steel fiber concrete can be obtained using Eq. (8) provided the coefficients (A, B, C, and D) can be obtained experimentally. To obtain A and B, the average maximum tensile strains (obtained from LVDTs) were plotted for each specimen as described in Fig. 6.

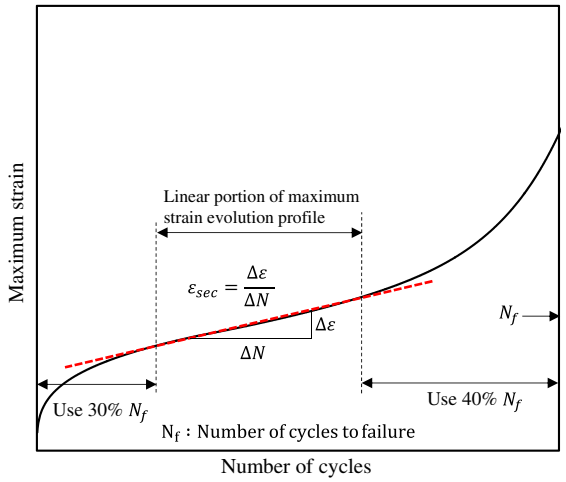

Fig. 6. Maximum strain versus number of fatigue loading cycles

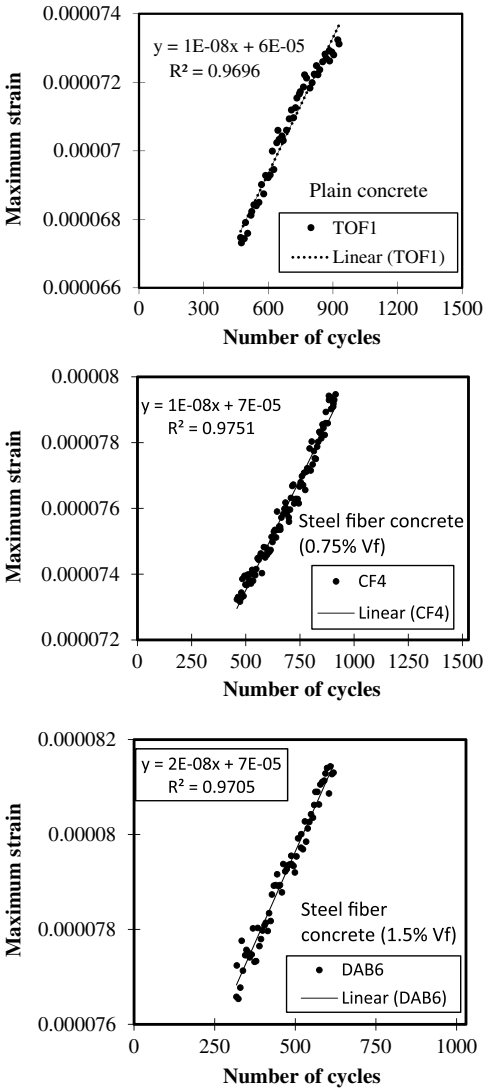

Fig. 7. Secondary strain rate for plain and steel fiber concrete

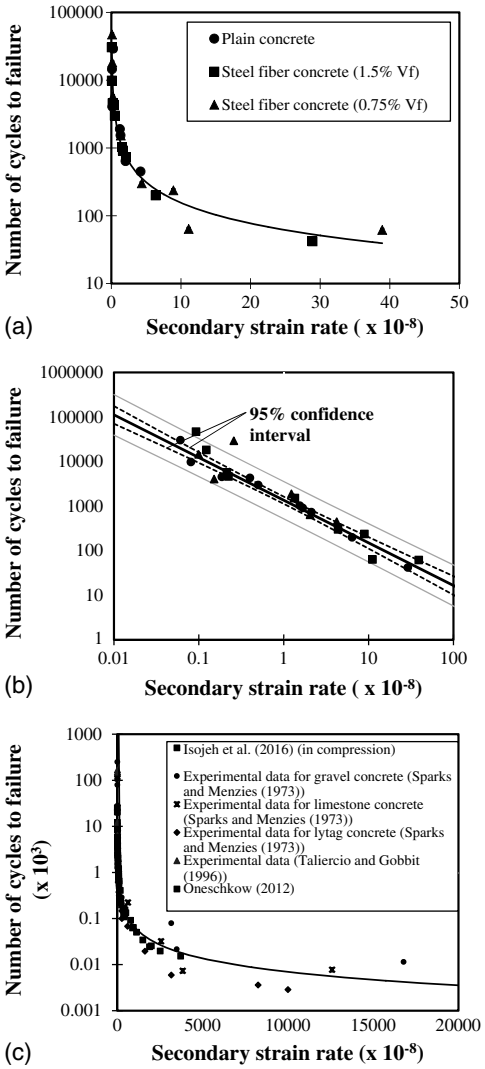

Fig. 8. Plot of number of cycles to failure against secondary strain rate

The secondary strain rates were obtained as the gradient of the plots (Fig. 7).

The correlation between the number of cycles to failure and the secondary strain rates was verified using the data from the specimens tested [Fig. 8(a)]. Because the frequency of loading used for plain and fiber reinforced concrete were similar, it was observed that all data points tend to fall along a given curve. The 95% confidence and prediction intervals are also shown in Fig. 8(b). Experimental data from previous investigations on the fatigue behavior of concrete in compression were plotted as shown in Fig. 8(c) (Sparks and Menzies 1973; Taliercio and Gobbit 1996; Oneschkow 2012; Isojeh et al. 2017). As observed, the profiles for the correlation between the number of cycles and the secondary strain rates are similar for concrete in tension and compression because both fit the power law curve.

Experimental data observed for the secondary strain rates and the number of cycles to failure for each specimen were plotted per steel fiber volume content in the form expressed in Eq. (3) (Fig. 9). From the plots, the values of A and B were obtained for plain and steel fiber reinforced concrete as the intercept and slope, respectively.

To obtain the values for parameters C and D, the maximum stress level per specimen was also plotted against the observed secondary strain rate as in Eq. (4) (Fig. 10). By substituting the values of A, B, C, and D into Eq. (8), the material parameters for plain and fiber reinforced concrete were obtained. The values for the material parameters are given in Table 3 for plain concrete, and for fiber concrete with 0.75 and 1.5% fiber volume content. As observed, the material parameter obtained for plain concrete is similar to that observed in the literature; hence, the approach developed for the determination of the material parameter (β) and the estimated parameters for steel fiber is reasonable.

The values of A, B, C, and D may vary depending on the loading parameters selected. However, for loading parameters different from those used in this investigation, the combination of the parameters (A, B, C, and D) in obtaining the material constant (β) in Eq. (8) will result in a value similar to the actual material constant in the Aas Jakobsen and Lenshow's linear model.

Damage Evolution for Steel Fiber Residual Strength and Secant Modulus

Modified damage evolution models have been proposed previously by the authors for concrete residual strength and fatigue secant modulus [Eq. (9)] (Isojeh et al. 2017). The models are functions of the maximum stress level, critical damage value, loading frequency, damage parameter s and material parameter β. The critical damage is the percentage reduction in concrete strength or fatigue secant modulus at failure. The values were reported to be 0.35 and

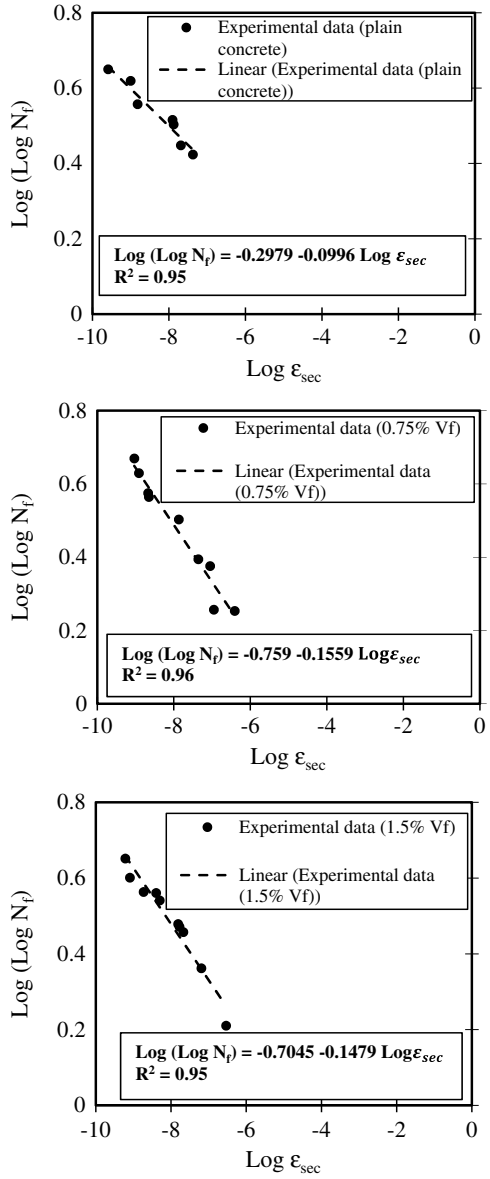

Fig. 9. Plot of $\mathrm{Log}(\mathrm{Log}N_f)$ versus Log $\varepsilon_{\mathrm{sec}}$

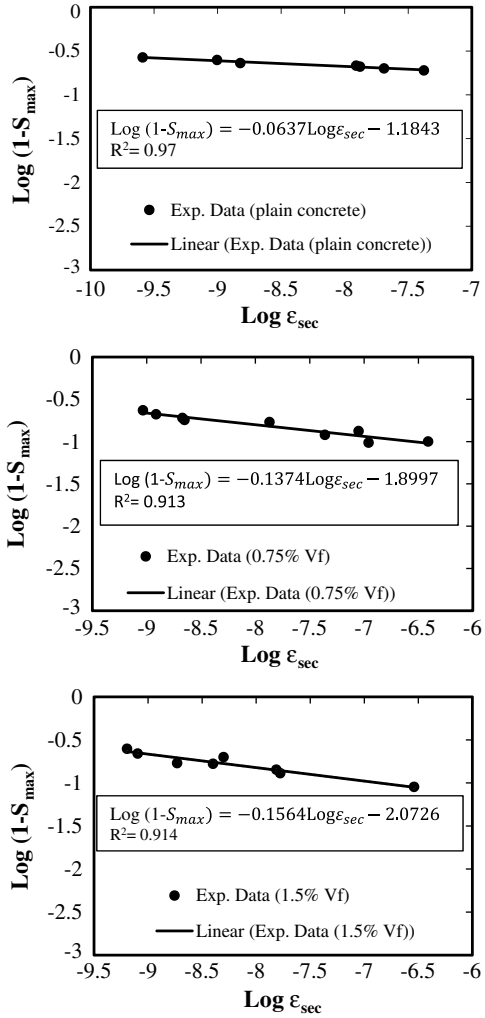

Fig. 10. Plot of $\mathrm{Log}(1 - S_{\mathrm{max}})$ versus Log $\varepsilon_{\mathrm{sec}}$

0.4 for concrete strength and fatigue secant modulus, respectively. Using these values for steel fiber concrete will give reasonable and conservative models

$$D = D_{cr} \exp\left[s\left(\frac{\Delta f}{f_c'} - C_f\right)\right] N^v \tag{9}$$

$$v = 0.434\ \mathrm{s}C_f[\beta(1-R)] \tag{10}$$

From Zhang et al. (1996) on influence of loading frequency

$$C_f = ab^{-\log f} + c \tag{11}$$

where N = number of cycles; s = damage parameter; D_{cr} = critical damage value; and C_f accounts for fatigue frequency.

Test data from Zhang et al. (1996) were used to obtain optimized values of the parameters (a, b, and c) in Eq. (11). These are given as 0.283, 0.941, and 0.715, respectively. The residual strength and fatigue secant modulus degradation can be estimated by substituting material parameter β for steel fiber concrete into the damage model.

Table 3. Material Parameter for Plain and Steel Fiber Reinforced Concrete

Fiber volume content % Vf	Coefficient A	Coefficient B	Coefficient C	Coefficient D	Material parameter β
0	−0.0996	−0.2979	−1.1843	−0.0637	0.0687
0.75	−0.759	−0.1559	−1.8997	−0.1374	0.0588
1.5	−0.7045	−0.1479	−2.0726	−0.1564	0.0470

The parameter s in the damage model depends on the stress ratio R and can be estimated from Fig. 11 for stress ratio values between 0 and 0.5. The damage evolution of plain and steel fiber reinforced concrete strength and fatigue secant modulus (0, 0.75, and 1.5% Vf) under fatigue loading at a maximum stress level of 0.8, stress ratio of zero, and a frequency of 5 Hz, are given in Fig. 12. As observed, the steel fiber volume content increased from 0 to 1.5% Vf, and the number of cycles leading to failure increased with corresponding delays in progressive damage.

Summary

Fatigue tests were conducted on steel fiber concrete to study the progressive behavior and to develop damage and material

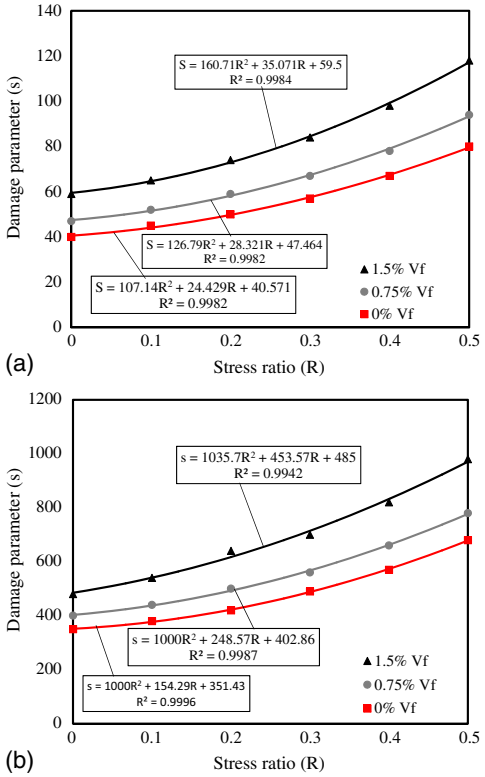

Fig. 11. (a) Damage parameter s for secant modulus of steel fiber; (b) residual strength of steel fiber

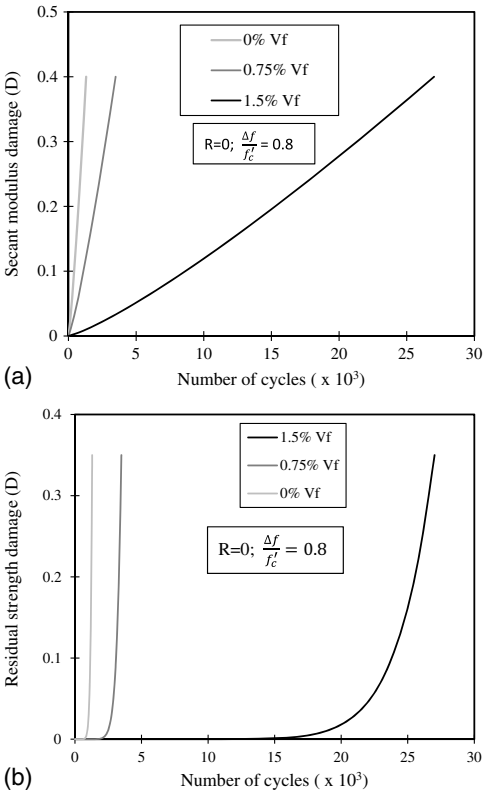

Fig. 12. (a) Residual strength; (b) fatigue secant modulus damage evolution for steel fiber concrete

parameters for steel fiber concrete under fatigue loading. To achieve this, a new concept was used to develop the required material parameters for plain and steel fiber reinforced concrete. From the comparison of the deformation evolution profiles in this investigation with those from compression fatigue tests in the literature, similarities were observed for tension and compression fatigue loading. Further, fatigue life increases as steel fiber volume content in concrete increases from 0 to 1.5%. The concept used in deriving the material parameter is appropriate because the value obtained for plain concrete agrees well with values in the literature. The damage models which incorporate the estimated material and damage parameters for steel fiber concrete can be implemented into constitutive models to enhance fatigue analyses of steel fiber concrete structures.

Acknowledgments

The authors gratefully acknowledge the Natural Science and Engineering Research Council (NSERC) of Canada and Hatch Ltd for the invaluable contributions and financial support to this research. The authors also acknowledge the assistance received from the Niger Delta Development Commission and the Delta State Government of Nigeria.

References

Aas-Jacobsen, K. (1970). "Fatigue of concrete beams and columns." *Bulletin No 70-1*, Institutt for Betonkonstruksjoner, Trondheim, Norway, 148.

Chang, D., and Chai, W. (1995). "Flexural fracture and fatigue behaviour of steel-fibre reinforced concrete structures." *Nucl. Eng. Des.*, 156(1–2), 201–207.

Chenkui, H., and Guofan, Z. (1995). "Properties of steel fibre reinforced concrete containing larger coarse aggregate." *Cem. Concr. Compos.*, 17(3), 199–206.

Cornelissen, H. A. W., and Reinhardt, H. W. (1984). "Uniaxial tensile fatigue failure of concrete under constant-amplitude and programme loading." *Mag. Concr. Res.*, 36(129), 216–226.

Cornelissen, H. A. W., and Reinhardt, H. W. (1986). "Effect of static and fatigue preloading on residual strength and stiffness of plain concrete." *6th Biennal European Conf. on Fracture—ECF6*, Amsterdam, Netherlands, 2087–2095.

FIB. (2010). *Model code for concrete structures*, Ernst & Sohn GmbH & Co., Berlin.

Guo, Z. (2014). *Principles of reinforced concrete: Fatigue resistance*, Elsevier, Oxford, U.K.

Holmen, J. O. (1982). "Fatigue of concrete by constant and variable amplitude loading." *ACI SP 75-4*, American Concrete Institute, Farmington Hills, MI, 71–110.

Isojeh, B., El-Zeghayar, M., and Vecchio, F. J. (2017). "Concrete damage under fatigue loading in uniaxial compression." *ACI Mater. J.*, 114(2), 225–235.

Maekawa, K., Toongoenthong, K., Gebreyouhannes, E., and Kishi, T. (2006). "Direct path-integral scheme for fatigue simulation of reinforced concrete in shear." *J. Adv. Concr. Technol.*, 4(1), 159–177.

Naaman, A. E., and Hammoud, H. (1998). "Fatigue characteristics of high performance fibre-reinforced concrete." *Cem. Concr. Compos.*, 20(5), 353–363.

Nanni, A. (1991). "Fatigue behaviour of steel fibre reinforced concrete." *Cem. Concr. Compos.*, 13(4), 239–245.

Oh, B. H. (1986). "Fatigue analysis of plain concrete in flexure." *ASCE J. Struct. Eng.*, 10.1061/(ASCE)0733-9445(1986)112:2(273), 273–288.

Oneschkow, N. (2012). "Influence of loading frequency on the fatigue behaviour of high-strength concrete." *Proc., 9th fib Int. Ph.D. Symp. in Civil Engineering*, Ernst & Sohn GmbH & Co., Berlin.

Petryna, Y. S., Pfanner, D., Stangenberg, F., and Kratzig, W. B. (2002). "Reliability of reinforced concrete structures under fatigue." *Reliab. Eng. Syst. Saf.*, 77(3), 253–261.

Ramakrishnan, V., Wu, Y. G., and Hossali, G. (1989). "Flexural fatigue strength, endurance limit and impact strength of fibre reinforced concretes." Transportation Research Board, Washington, DC.

Singh, S. P., and Kaushik, S. K. (2001). "Flexural fatigue analysis of steel fibre-reinforced concrete." *ACI Mater. J.*, 98(2), 306–312.

Sparks, P. R., and Menzies, J. B. (1973). "The effect of rate of loading upon the static and fatigue strength of plain concrete in compression." *Mag. Concr. Res.*, 25(83), 73–80.

Taliercio, A. L. F., and Gobbit, E. (1996). "Experimental investigation on the triaxial fatigue behaviour of plain concrete." *Mag. Concr. Res.*, 48(176), 157–172.

Tepfers, R. (1979). "Tensile fatigue strength of plain concrete." *ACI J.*, 76(8), 919–933.

Tepfers, R., and Kutti, T. (1979). "Fatigue strength of plain, ordinary, and lightweight concrete." *ACI J.*, 76(5), 635–652.

Torrenti, J. M., et al. (2010). *Mechanical behaviour of concrete*, Wiley, Chichester, U.K., 185–223.

Vega, I. M., Bhatti, M. A., and Nixon, W. A. (1995). "A nonlinear fatigue damage model for concrete in tension." *Int. J. Damage Mech.*, 4(4), 362–379.

Zhang, B., Phillips, D. V., and Wu, K. (1996). "Effects of loading frequency and stress reversal on fatigue life of plain concrete." *Mag. Concr. Res.*, 48(177), 361–375.

Zhang, J., Stang, H., and Li, V. C. (1999). "Fatigue life prediction of fibre reinforced concrete under flexural load." *Int. J. Fatigue*, 21(10), 1033–1049.